

Design, synthesis, and evaluation of substituted 6-amide-4-anilinoquinazoline derivatives as c-Src inhibitors

Cite this: *RSC Adv.*, 2013, **3**, 26230

Fei Fang,^{†a} Dong-Dong Li,^{†a} Jing-Ran Li,^a Jian Sun,^a Qian-Ru Du,^a Hai-Bin Gong^{*b} and Hai-Liang Zhu^{*a}

The 4-anilinoquinazoline scaffold has been historically used for designing EGFR/VEGFR/HER2 inhibitors while it has not been reported widely for developing c-Src inhibitors. Thus, a series of novel 4-anilinoquinazoline derivatives grafting different amide moieties at the 6-position were designed and synthesized as potential inhibitors for c-Src. In this manuscript, all of the designed compounds were screened *via* molecular docking using Discovery Studio 3.5 software. As expected, the results of the docking study revealed that most of these targeted compounds possessed lower binding energy than the positive control Saracatinib. Subsequently, all of the screened compounds were synthesized and evaluated for their c-Src *in vitro* inhibitory activities and *in vitro* antiproliferation assays against four human cancer cells (A549, MCF-7, HepG-2, HeLa). Among these compounds, **24** exhibited the most potent inhibitory activity against c-Src kinase as well as at the cellular level, of which the IC₅₀ value reached up to 2.9 nM, comparable to the positive compound Saracatinib. Kinase selectivity profile also demonstrated that compound **24** showed good selectivity over several close kinase targets. These results, along with relative 3D-QSAR study, could provide an important basis for further development of compound **24** as a potent tyrosine kinase inhibitor.

Received 18th September 2013

Accepted 23rd October 2013

DOI: 10.1039/c3ra45204b

www.rsc.org/advances

1. Introduction

Currently there are about 500 protein kinases which constitute almost 2% of the human genome,^{1,2} most of which are closely involved in several important cellular responses such as proliferation, migration, survival, cell cycle progression and specialized cell signals.^{3–5} c-Src tyrosine kinase is the prototypical member of SFKs (Src family kinases) of non-receptor protein tyrosine kinases,^{6,7} which transfer the γ -phosphate moiety of ATP to the phosphorylation of phenolic group of tyrosine residue on substrate proteins.^{8,9} A number of reports revealed that c-Src could play a critical role in a series of the function of organism, such as cell transformation, mitogenesis, differentiation, and oncogenesis.^{10–12} In contrast to its highly controlled expression in normal cells, mounting evidence disclosed that overexpression and/or coexpression of c-Src has been implicated in numerous of tumor types (colon, breast, ovarian, head and neck)^{6,8,10} and involved in poor prognosis of the patients. Research around increased activity of c-Src has revealed that deregulation of the enzyme can be linked to

increased motility/invasiveness of tumor cells and to tumor progression.^{13,14} Moreover, as a result of extensive preclinical studies, metastatic bone disease with aberrant c-Src kinase activity occurs in many solid tumor cancers.^{15–17} In recent publications, one new hypothesis^{18,19} could be utilized to explain the association between c-Src and cancers that the irregularity of c-Src tyrosine kinase predominantly leads to alterations of cell adhesion and cytoskeletal, ultimately resulting in a change to a motile, invasive phenotype. Therefore there is still much of interest in developing the c-Src tyrosine kinase and evaluating small molecule c-Src inhibitors to prohibit the growth of a variety of cancers.

Fig. 1 shows that several known c-Src kinase inhibitors²⁰ have been identified to date. It is noteworthy that these compounds generally employ three main scaffolds:²¹ 4-anilinoquinazolines,²² dihydropyrimido-quinolinones,²³ and pyrazolo-pyrimidines.²⁴ The most potent compound, exemplified by Bosutinib (SKI-606),^{6,20} as a novel, dual Src/Abl inhibitor with IC₅₀ values of 1.2 nM and 1 nM, respectively, has been approved to cure metastatic breast cancer and chronic myelogenous leukemia by FDA last year, demonstrating that the 4-anilinoquinoline-3-carbonitrile template possesses high selectivity as Src inhibitor. However, there are many developing compounds showing poor *in vivo* activity or only exhibit high potency in some limited metastasis models, partially due to itself poor solubility or pharmacokinetics properties.²¹ In addition, there are also some

^aState Key Laboratory of Pharmaceutical Biotechnology, Nanjing University, Nanjing 210093, P. R. China. E-mail: zhuhl@njnu.edu.cn; Fax: +86-25-8359 2672; Tel: +86-25-8359 2572

^bXuzhou Central Hospital, Xuzhou 221009, P. R. China. E-mail: ghbxzh@126.com

[†] These authors contributed equally to this work.

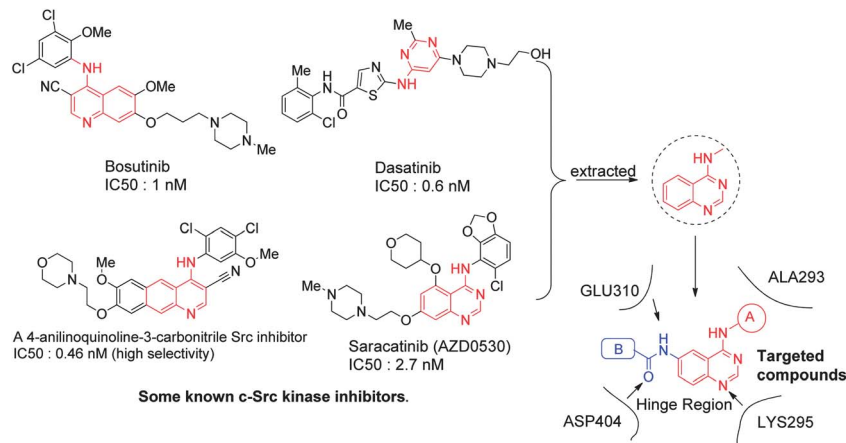


Fig. 1 Some known c-Src kinase inhibitors.

side effects (skin rash, gastro-intestinal, pleural effusions, cytopenia), toxicities and drug-resistance reported under the clinical trial of candidates.^{21,25} Therefore, the pursuit of novel c-Src inhibitors with a better anti-tumor effects and more safety profile is still the main issue today.

As is known to all that the 4-anilinoquinazoline drugs such as Gefitinib,^{26,27} Erlotinib,²⁸ and Saracatinib²⁰ have possessed a good kinase selectivity profile, mainly due to the iterative modification of the 4-anilinoquinazoline skeleton. From a number of experimental data and molecular modeling studies focusing on the c-Src kinase inhibition,^{29,30} it is disclosed that the nitrogen at position 1 and 3 of the anilinoquinazoline ring is significant for c-Src inhibitory potency, and the binding potency could be enhanced by the replacement of electron-donating substituents at 6- and 7- positions. Taken together, a series of novel small molecules elaborated around 4-anilinoquinazoline scaffold were designed. In our previous study,³¹ the modification of 6-position of the quinazoline ring could enhance the binding potency as protein kinase inhibition. Herein, these 4-anilinoquinazoline derivatives in this manuscript would still focus on the replacement at the 6-position of the quinazoline ring with various heterocyclic ring moiety. Subsequently, in order to verify whether these compounds we designed could bind tightly to our target protein c-Src active domain, we have performed molecular docking^{32–35} to study the interaction between these novel 4-anilinoquinazoline analogs and the protein–ligand complex (PDB code: 3F3V), retrieved from the RCSB Protein Data Bank, by the means of the CDOCKER protocol in the Accelrys Discovery Studio 3.5 suite (Accelrys Software Inc.). Compared with the positive drug Saracatinib, most of the designed molecules (except compound 7, 8, 10, 13, 15, 18, 20) possessed lower interaction energy, demonstrating that they were likely to exhibit more potency as c-Src inhibitors (Fig. 2).

In this present study, we would provide the synthetic methods of this series of novel small molecules, and discuss carefully the structure–activity relationship (SAR) of compounds as antitumor agents. Additionally, we also built the relative 3D-QSAR model based on the SAR of these 4-anilinoquinazoline

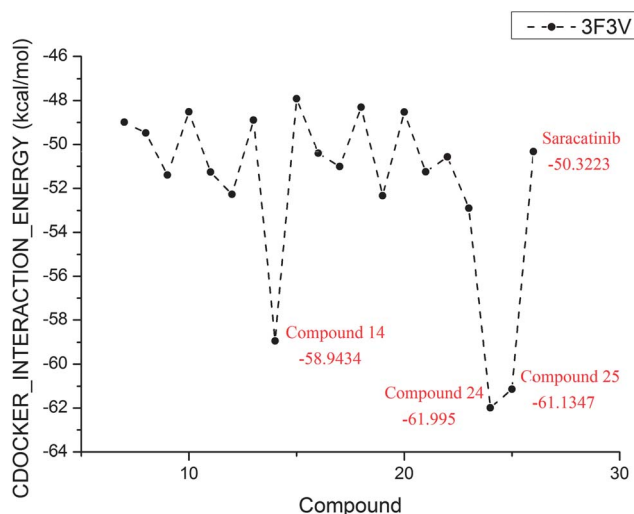


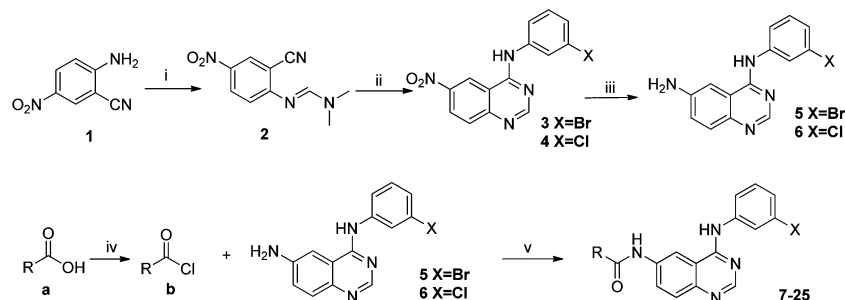
Fig. 2 The CDOCKER_INTERACTION_ENERGY (kcal mol⁻¹) obtained from the docking study of the targeted compounds by the CDOCKER protocol (Discovery Studio 3.5, Accelrys, Co. Ltd).

derivatives, which maybe rationalize the experimental observations and guide us to screen good potency c-Src inhibitors in the further study.

2. Results and discussion

2.1. Chemistry

Nineteen 4-anilinoquinazoline derivatives were screened by molecular docking and synthesized in aim to evaluate their biological activity. Herein, the rapid process to synthesize the 4-anilinoquinazoline intermediates (compound 5 and 6) with amino group at the 6-position was depicted as Scheme 1. As previously reported,³¹ 6-amino-4-anilinoquinazoline (compound 5 and 6) could be easily obtained in two steps from the starting material 2-amino-5-nitrobenzonitrile. Subsequently seen in Scheme 1, benzoic acid and phenylacetic acid with different substituents (a) were refluxed with thionyl chloride to give the corresponding acyl



Scheme 1 Synthesis of 6-amide-4-anilinoquinazoline derivatives. Reagents and conditions: (i) DMF-DMA/reflux; (ii) $\text{ArNH}_2/\text{AcOH}/\text{reflux}$; (iii) $\text{Fe}/\text{AcOH}/\text{EtOH}/\text{H}_2\text{O}/\text{reflux}$; (iv) thionyl chloride/reflux; (v) $\text{EtOAc}/\text{K}_2\text{CO}_3/0^\circ\text{C}$.

chloride (**b**). After chlorination, 4-anilinoquinazoline scaffold (compound **5** and **6**) was dropwise added into a solution of acyl chloride (**b**) and potassium carbonate dissolved in ethyl acetate, leading to finally generate the corresponding amide analogues **7–25**.

The above of all compounds have been purified by different favorable experimental methods, such as extraction, chromatography and recrystallization. Additionally, all the synthetic compounds have been presented both satisfactory analytic and spectroscopic data, which were in full accordance with their depicted structures.

2.2. Bioassay

2.2.1. c-Src enzyme assay. All synthesized compounds have been evaluated for their c-Src inhibitory activity and the obtained results (Table 1) presented their activity data depicted as IC_{50} values (the half maximal inhibitory concentration of c-Src mediated autophosphorylation). As expected, most of these compounds showed moderate inhibitory activities for the target protein kinase. In particular, compound **24**, which IC_{50} value can reach up to 2.9 nM, was identified as the most potent c-Src inhibitor. For better understanding and comparing with each other, these results were plotted as a line-scatter graph presented in Fig. 3. In the light of steric and electronic factors employed by the targeted compounds, the general structure-activity relationships (SAR) would be discussed. Initially, compounds (**11**, **12**, **13**) with the Br substituent located at the *para* position of the 4'-aniline ring showed roughly similar inhibitory activities with those with the Cl atom (**21**, **22**, **23**). Then the compounds (**14**, **24**) containing pyridine ring at the 6-position of the quinazoline ring exhibited obviously more potent inhibitory activities than the rest compounds with benzene ring. It resulted from pyridine ring with more hydrophilic potency. It was also concluded that the amide formed by phenylacetic acid (compound **11–14**) at the 6-position slightly improved the c-Src inhibitory activity compared to a relatively benzoic acid substituent (compound **7–8**), resulting from the longer C-chain with more hydrophilic potency. From compound **11**, **12**, **13**, inferring that those compounds with stronger electronegativity substitutes of heterocyclic ring acids led to a noteworthy loss of activity ($4\text{-Br} > 4\text{-Cl} > 4\text{-F}$). Particularly, compound **25** that possessed 3,4-diethoxy substituents

performed better than the others (**18**, **19** and **20**). This indicated that the disubstituted inhibitors were likely to be superior for inhibitory potency of c-Src kinase to monosubstitutions. Taken together, based on the results above, compound **24**, along with **14** and **25**, could be selected as potential c-Src inhibitors and antitumor agents for further optimization.

Moreover, an acute oral toxicity test was conducted with mice to determine the toxicity from a single dose *via* the oral route. Based on the results of study (not listed), the single dose acute oral LD_{50} (half maximal concentration of lethal doses) values of the most potent compound **24** is greater than 5000 mg kg^{-1} of body weight.

2.2.2. Antiproliferation assay. The target compounds were also evaluated in *in vitro* antiproliferation assays against four human cancer cells: HepG-2, MCF-7, A549 and HeLa. The HepG-2 and MCF-7 were known to be relative with c-Src family. Meanwhile, to control for non-specific cytotoxicity, compounds were evaluated against A549 cells and HeLa cells. The obtained results were listed in Table 2. As expected, all targeted compounds showed moderate potent inhibitory activities against HepG-2 and MCF-7. Surprisingly, the A549 cells and HeLa cells were also good targets that belong to these quinazoline derivatives. In accordance with the c-Src kinase assay, three compounds (**24**, **25**, **14**) with the level of IC_{50} values less than $1 \mu\text{M}$, performed better than the other compounds in the cellular level, comparable with the positive compound Saracatinib. In addition, the most potent small molecule **24** ($\text{IC}_{50} = 0.55, 0.34, 0.41, 0.67 \mu\text{M}$, respectively) even showed more potent inhibition than Saracatinib in some of these four cells.

2.3. The kinase selectivity assay

The kinase selectivity profile of this series was assessed, using compound **24** as a representative. The obtained results (Table 3), presented their activity data depicted as IC_{50} values. Interestingly, compound **24** showed moderate inhibitory activities for the majority of these target protein kinases, which belong to tyrosine and serine/threonine kinase. In addition, compound **24** performed better as c-Src inhibitors than against another two kinases. These results could provide sufficient evidence compound **24** could be selected as potential c-Src inhibitors and antitumor agents for further optimization.

Table 1 Enzyme activities (IC_{50} , nM) of compounds **7–25** against human c-Src kinases

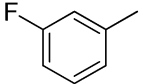
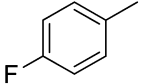
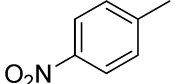
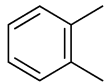
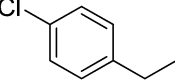
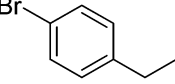
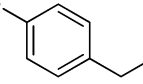
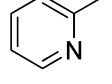
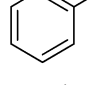
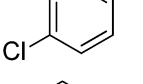
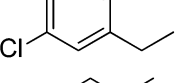
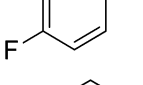
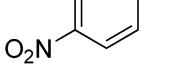
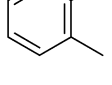
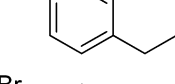
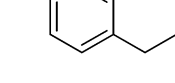
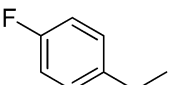
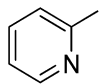
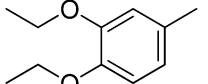
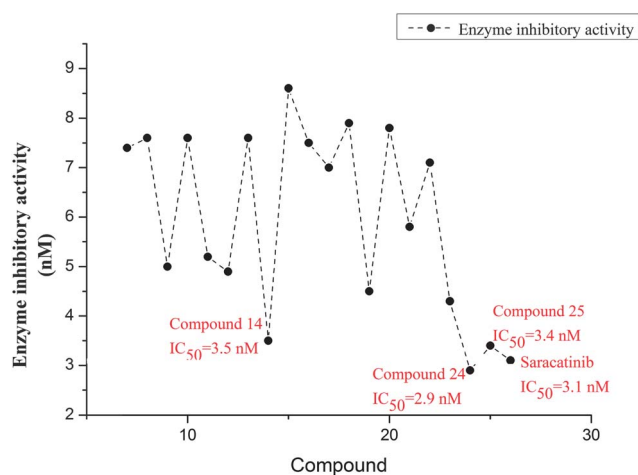
Compound	R	X	c-Src \pm SD (μ M)
7		Br	44 ± 1.78
8		Br	76 ± 3.01
9		Br	59 ± 2.14
10		Br	76 ± 2.97
11		Br	56 ± 2.23
12		Br	49 ± 1.63
13		Br	76 ± 2.31
14		Br	3.5 ± 0.25
15		Br	120 ± 4.53
16		Br	95 ± 3.56
17		Br	70 ± 1.97
18		Cl	79 ± 2.84
19		Cl	45 ± 1.58
20		Cl	78 ± 2.93
21		Cl	58 ± 2.07
22		Cl	71 ± 2.81

Table 1 (Contd.)

Compound	R	X	c-Src \pm SD (μ M)
23		Cl	43 ± 1.64
24		Cl	2.9 ± 0.17
25		Cl	3.4 ± 0.27
Saracatinib	—	—	3.1 ± 0.12

**Fig. 3** Inhibitory activity of compounds **7–25** against c-Src protein kinases were represented as a line-scatter graph.

2.4. Molecular docking

Docking study was performed to evaluate the binding potency between compound **24**, Saracatinib and the active domain of the c-Src kinase (PDB code: 3F3V). The obtained results were depicted clearly by the following two pictures (Fig. 4). Fig. 4A and C showed the 2D and 3D binding mode of the compound **24** interacting with 3F3V protein, respectively. The model also depicted that extensive hydrophobic interactions were formed between compound **24** and residues Val 281, Ala 293, Lys 295, Met 314, Val 323, Thr 338, Leu 393, Ala 403 and Phe 405 of the ATP-binding pocket of c-Src kinase (Fig. 4A). From Fig. 4C and D, there were only one H-bonds formed between the reference compound Saracatinib and 3F3V, whereas four H-bonds were formed between compound **24** and 3F3V, inferring that the candidate was more tightly embedded into the ATP binding pocket than Saracatinib. Insight into Fig. 4C, four amino acids Lys 295, Glu 310, Asp 404, Phe 405 located in the binding pocket of protein were significant for the conformation with compound **24**, which were stabilized by three π -cation bonds and three hydrogen bonds (one interaction with amino acid

Table 2 *In vitro* anticancer activities (IC₅₀, μM) against four human tumor cell lines

Compound	IC ₅₀ ± SD (μM) ^a			
	HEPG-2 ^b	MCF-7 ^b	HeLa ^b	A549 ^b
7	6.38 ± 0.51	8.49 ± 0.61	9.35 ± 0.74	10.87 ± 1.03
8	9.13 ± 0.83	7.65 ± 0.68	10.35 ± 0.92	11.43 ± 0.93
9	7.43 ± 0.64	6.84 ± 0.49	9.63 ± 0.97	8.69 ± 0.73
10	8.41 ± 0.79	7.73 ± 0.57	9.29 ± 0.87	9.39 ± 0.85
11	7.38 ± 0.66	8.47 ± 0.72	6.48 ± 0.44	10.59 ± 0.86
12	6.36 ± 0.33	7.84 ± 0.64	7.69 ± 0.57	9.34 ± 0.48
13	7.92 ± 0.55	8.14 ± 0.57	11.47 ± 1.32	9.39 ± 0.74
14	0.88 ± 0.56	0.49 ± 0.12	1.03 ± 0.08	0.93 ± 0.19
15	9.49 ± 0.89	12.44 ± 1.48	10.62 ± 1.07	11.38 ± 1.73
16	8.69 ± 0.76	10.48 ± 1.09	9.39 ± 0.84	9.73 ± 0.74
17	6.39 ± 0.53	7.49 ± 0.64	6.15 ± 0.64	7.78 ± 0.75
18	7.36 ± 0.53	9.33 ± 0.74	8.95 ± 0.53	9.59 ± 0.78
19	3.43 ± 0.23	4.32 ± 0.47	6.58 ± 0.51	4.97 ± 0.47
20	6.59 ± 0.58	8.40 ± 0.73	7.93 ± 0.51	8.39 ± 0.68
21	8.62 ± 0.76	7.40 ± 0.53	10.04 ± 0.79	8.85 ± 0.65
22	6.19 ± 0.37	5.53 ± 0.39	8.69 ± 0.59	7.69 ± 0.53
23	4.67 ± 0.39	5.89 ± 1.56	3.25 ± 1.43	7.38 ± 0.16
24	0.55 ± 0.13	0.34 ± 0.09	0.41 ± 0.14	0.67 ± 0.06
25	0.72 ± 0.21	0.63 ± 0.26	0.79 ± 0.18	0.93 ± 0.43
Saracatinib	0.50 ± 0.06	0.49 ± 0.02	0.67 ± 0.05	0.61 ± 0.03

^a Antiproliferation activity was measured using the CCK8 assay. Values are the average of two independent experiments. ^b Cancer cells kindly supplied by KeyGen Biotech; HepG-2 (hepatocellular liver carcinoma cell line), MCF-7 (breast cancer), HeLa (immortal cell line) and A549 (carcinomic human alveolar basal epithelial cell).

Table 3 IC₅₀ datas for compound **24** against several related kinases screened

Kinase	IC ₅₀ (nM)	Fold selectivity
c-Src	2.9	—
EGFR	97	33
CDK2	837	289
PTK2	452	156
JAK2	961	331

side-chains; two interactions with amino acid main-chains). Two Pi-cation bonds were formed between amino acid Lys 295 and quinazoline ring of compound **24** with their lengths 5.5 Å and 6.2 Å, respectively; the other one with its length 6.9 Å was formed between amino acid Phe 405 and N of amide chain. There are two hydrogen bonds between amino acid Asp 404 and N, O of amide chain, with their lengths 1.9 Å and 2.3 Å, respectively; another one with 2 Å was formed between amino acid Glu 310 and the N atom of amide chain. Besides, the bromine and chlorine of 4-aniline head could contribute to stabilizing the binding complex, derived from the previous discussion.³¹ These results could provide a molecular level foundation for **24** as the most potent c-Src inhibitor.

2.5. 3D QSAR model

In order to obtain a kind of systematic SAR profile based on 6-amide-4-anilinoquinazoline analogues as antitumor agents and to explore the more potent and selective c-Src inhibitor,

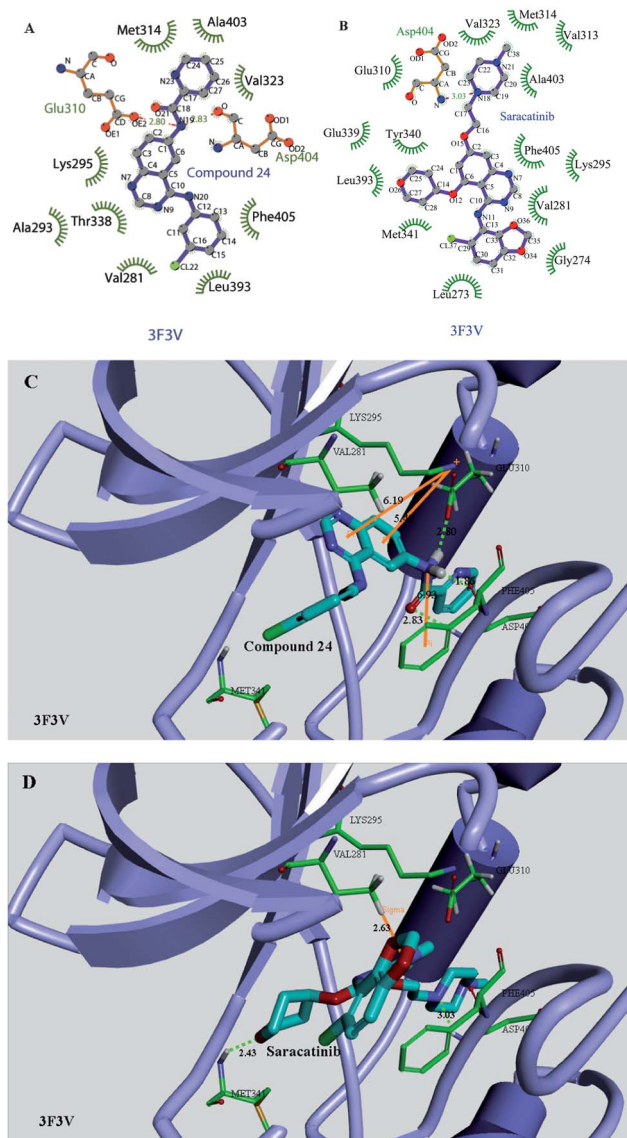


Fig. 4 The two kinds of binding modes between the active conformation of compound **24** and the target protein c-Src (PDB code: 3F3V) provided by the CDocker protocol (Lingar and Discovery Studio 3.5, Accelrys, Co. Ltd). (A) 2D molecular docking model of compound **24** with 3F3V. (B) 2D molecular docking model of Saracatinib with 3F3V. (C) The 3D interaction map between compound **24** and the c-Src protein. (D) The 3D interaction map between Saracatinib and the c-Src protein.

3D-QSAR model was performed by using the corresponding pIC₅₀ values which were converted from the obtained IC₅₀ (nM) values of c-Src kinase inhibition and performed by built-in QSAR software of DS 3.5 (Discovery Studio 3.5, Accelrys, Co. Ltd). The way of this transformation was derived from an online calculator developed from an Indian medicinal chemistry lab (<http://www.sanjeevslab.org/tools-IC50.html>). The training and test set was divided by the random diverse molecules method of DS 3.5, in which the test set accounts for 80% while the training set was set to 20%. The 19 target compounds were divided into two parts: 15 agents as training set and the rest 4 agents as relative test set, which had been presented in Table 4. An efficient solution in this research depended on docking study and

Table 4 Experimental, predicted inhibitory activity of compounds **7–25** against c-Src by 3D-QSAR models based on active conformations selected from the preliminary molecular docking study

Compound	c-Src kinase inhibition		Residual error
	Actual pIC ₅₀ ^b	Predicted pIC ₅₀	
7	7.13	7.01	0.1213
8	7.12	7.12	−0.0021
9	7.23	7.10	0.1309
10	7.12	7.17	−0.0518
11 ^a	7.07	7.24	−0.1690
12	7.31	7.31	0.0027
13	7.12	7.16	−0.0383
14 ^a	8.46	8.49	0.0031
15	6.92	7.03	−0.1062
16 ^a	7.13	7.08	0.0492
17	7.16	7.12	0.0328
18	7.10	7.08	0.0183
19	7.35	7.36	−0.0098
20	7.11	7.08	0.0297
21 ^a	7.24	7.28	−0.0387
22	7.15	7.22	−0.0696
23	7.37	7.37	−0.0069
24	8.54	8.49	0.0497
25	8.47	8.57	−0.1007

^a Compounds were selected as the test sets while the rest ones were in the training sets. ^b The IC₅₀ values of the compounds against c-Src (Table 1) were converted into pIC₅₀ values by using the online calculator (<http://www.sanjeevslab.org/tools-IC50.html>).

the reliability of this method has been documented in previous studies.

In default situation, the alignment conformation of each molecule was the one that filtered the lowest CDOCKER_INTERACTION_ENERGY among the twenty docked poses. The 3D-QSAR model defined the critical regions (steric or electrostatic) affecting the binding affinity, generated from DS 3.5. It was a PLS model built on 400 independent variables (conventional $r^2 = 0.883$). The observed and predicted values and corresponding residual values for the training set and test set molecules in 3D-QSAR model were presented in Table 4. Moreover, their graphical relationship had been illustrated in Fig. 5A, in which the plot of the observed IC₅₀ versus the predicted values demonstrated that this model could be used in prediction of activity for novel 4-anilinoquinazoline derivatives as c-Src inhibitor.

The contour plot of the electrostatic field region favorable (in blue) or unfavorable (red) for anticancer activity based on c-Src protein target were shown in Fig. 5B while the energy grids corresponding to the favorable (in green) or unfavorable (yellow) steric effects for the c-Src affinity were shown in Fig. 5C. It was widely acceptable that a better inhibitor based on the 3D QSAR model should have strong van der Waals attraction in the green areas and a polar group in the blue electrostatic potential areas (which were dominant close to the skeleton). Thus, this promising model would provide a guideline to design and optimize more effective c-Src inhibitors based on the 4-anilinoquinazoline analogues skeleton and pave the way for us to further study in future.

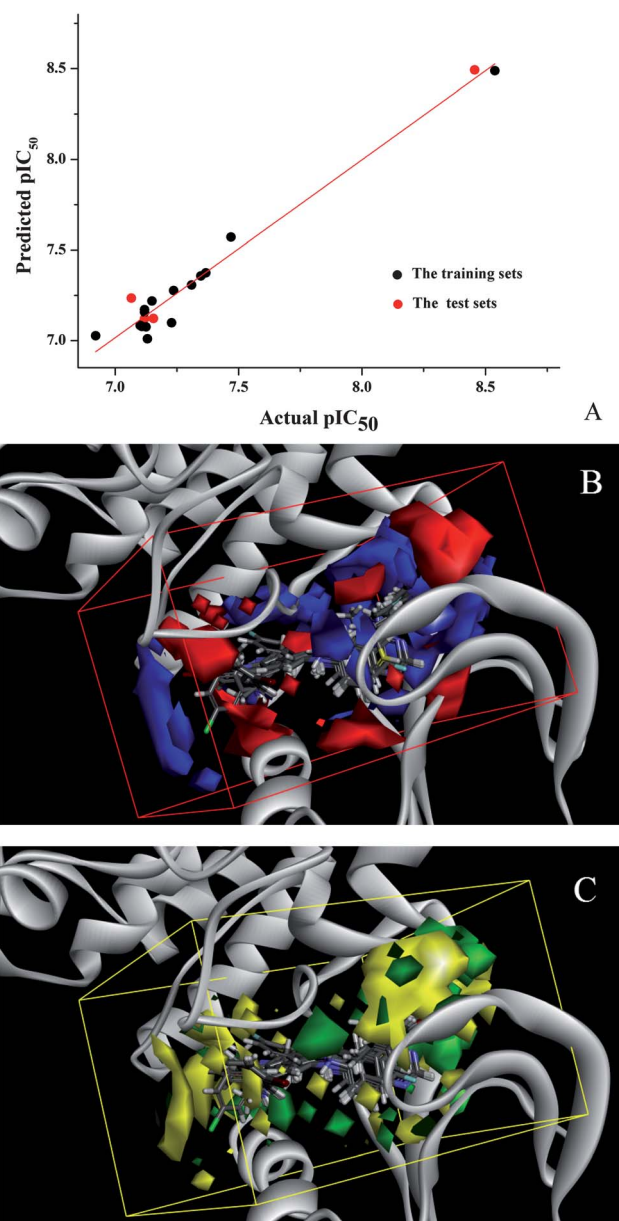


Fig. 5 (A) The predicted versus experimental pIC₅₀ values for the inhibition of c-Src (PDB: 3F3V). (B) Isosurface of the 3D-QSAR model coefficients on electrostatic potential grids. The blue triangle mesh represents positive electrostatic potential and the red area represents negative electrostatic potential. (C) Isosurface of the 3D-QSAR model coefficients on van der Waals grids. The green triangle mesh representation indicates positive coefficients; the yellow triangle mesh indicates negative coefficients.

3. Conclusion

In summary, a series of 6-amide-4-anilinoquinazoline analogues have been synthesized and showed modest potency against c-Src, with IC₅₀ values ranging from single-digit nanomolar to a hundred nanomolar. Among these small molecules, compound **24** displayed the most potent activity against c-Src (IC₅₀ = 2.9 nM), being comparable with the positive control Saracatinib (IC₅₀ = 3.1 nM). The docking results indicated that compound **24** could bind well inside the active site of c-Src.

These results, along with molecular docking observations, are significant evidence to demonstrate the compound **24** could be optimized as a potential c-Src inhibitor in the further study. Moreover, a new 3D QSAR model was built with the activity data and binding conformations to check the previous work as well as to provide us cogent foundation and new ideas about further design and modification.

4. Experimental section

4.1. Materials and methods

All of the synthesized compounds were assessed by thin layer chromatography (TLC), proton nuclear magnetic resonance (^1H NMR) and elemental microanalyses (CHN). ^1H NMR spectra were measured on a Bruker AV-300 or AV-500 spectrometer with tetramethylsilane (TMS) as an internal reference ($\delta = 0$) at 25 °C. Chemical shifts are reported in parts per million (ppm) using the residual solvent line as internal standard. Splitting patterns are designed as s, singlet; d, doublet; t, triplet; m, multiplet. ESI-MS spectra were recorded on a Mariner System 5304 Mass spectrometer. Elemental analyses were performed on a CHN-O-Rapid instrument and were within $\pm 0.4\%$ of the theoretical values. Melting points were determined on a XT4 MP apparatus (Taike Corp., Beijing, China) and are as read. Analytic thin-layer chromatography (TLC) was performed on the glass-backed silica gel sheets (silica gel 60 Å GF254). All compounds were detected using UV light (254 nm or 365 nm).

4.2. General method for the preparation of compounds 5, 6 (Scheme 1)

N-4-(3-Bromophenyl)quinazoline-4,6-diamine (**5**) or *N*-4-(3-chlorophenyl)quinazoline-4,6-diamine (**6**) could be obtained according to the previous publications.³¹ 5-Nitro-anthranilonitrile **1** (4.89 g, 30 mmol, 1.0 equiv.) was dissolved in dimethylformamide dimethyl acetal (10 mL) and the mixture was refluxed (70–80) °C for 2 h. After the resulting mixture cooling to room temperature for 2–3 h and then the yellow compound was filtered, washed with ethyl ether and dried to give **2** (yield: 80–90%). The compound **2** was suspended in 3-chloroaniline (1.1 equiv.) or 3-bromoaniline (1.1 equiv.) and then the mixture was heated and stirred at reflux in acetic acid (20 mL) for 2 h. The yellow precipitate that formed was filtered hot, washed with hot acetic acid, diethyl ether, and dried to give the desired nitroquinazoline **3** or **4** (yield: 80–90%). 6-Nitroquinazoline **4** (2.0 g, 6.65 mmol, 1.0 equiv.), iron (2.5 g, 45 mmol, 6.7 equiv.) and acetic acid (6 mL, 90 mmol, 13.5 equiv.) were suspended in aqueous ethanol (180 mL, 77.8% v/v) and refluxed (70–80 °C) for 5–6 h. After the reaction mixture cooling to room temperature, concentrated ammonia (40 mL) was added. The resulting solid was extracted with ethyl acetate for column chromatography. Column chromatography was performed using silica gel (200–300 mesh) eluting with ethyl acetate and petroleum ether (3 : 1, v/v) to give amine **6** (yield: 50–60%). m.p. 163–164 °C; ^1H NMR (300 MHz, DMSO- d_6 , δ ppm): 4.08 (s, 2H, NH₂), 6.93 (s, 1H), 7.13 (d, $J = 7.86$, 2H), 7.24 (dd, $J_1 = 11.13$ Hz, $J_2 = 8.97$ Hz, 1H), 7.33 (s, $J = 8.06$ Hz, 1H),

7.59 (d, $J = 7.68$ Hz, 1H), 7.78 (d, $J = 8.97$ Hz, 1H), 7.94 (s, 1H), 8.65 (s, 1H, NH). ESI-MS: 271.1 (C₁₄H₁₁ClN₄, [M + H]⁺). Anal. calcd for C₁₄H₁₀ClN₄: C, 62.11%; H, 4.10%; N, 20.70%. Found: C, 61.93%; H, 4.36%; N, 21.07%. *N*-4-(3-Bromophenyl)quinazoline-4,6-diamine (**5**) was also prepared as described for **6**.

4.3. General procedure for the synthesis of a, b and 7–25 (Scheme 1)

The starting materials (**a**) for the synthesis of amides should be activated in the first procedure: acid (100 mg) and SOCl₂ (6–10 mL) were mixed and stirred at reflux (80 °C) for 4 hours. The reaction mixture was cooled and evaporated to give reactive acyl chloride (**b**) obtained as an oil, which would be dissolved in ethyl acetate (5–6 mL) in the next step.

A solution of acyl chloride dissolved with ethyl acetate was added dropwise to compound **5** or **6** (0.5 mM) in ethyl acetate containing potassium carbonate (300 mg) at 0 °C with constant stirring overnight. The reaction mixture was then poured in excess of diluted NaOH and extracted with EtOAc. The extraction liquid was purified by a flash chromatography with EtOAc-petroleum ether (3 : 1, v/v) to give these amides as follows: the yields were about between 30 and 60%.

4.3.1. *N*-4-((3-Bromophenyl)amino)quinazolin-6-yl)-3-fluorobenzamide (7). Yellow powder, yield: 82%. m.p. 250–252 °C; ^1H NMR (300 MHz, DMSO- d_6 , δ ppm): 7.28–7.43 (m, 4H), 7.59–7.66 (m, 1H), 7.75 (t, $J = 3.00$ Hz, 1H), 7.85 (t, $J = 5.09$ Hz, 2H), 7.76 (dd, $J_1 = 8.97$ Hz, $J_2 = 8.97$ Hz, 1H), 8.17 (s, 1H), 8.31 (s, 1H), 8.61 (s, 1H), 8.90 (s, 1H), 9.98 (s, 1H), 10.74 (s, 1H). ^{13}C NMR (300 MHz, DMSO- d_6) δ : 168.45, 163.85, 158.28, 153.34, 149.46, 144.53, 137.43, 133.46, 130.05, 129.53, 127.45, 124.76, 124.52, 120.78, 120.52, 115.80, 114.75, 114.23. ESI-MS: 438.2 (C₂₁H₁₅BrFN₄O [M + H]⁺). Anal. calcd for C₂₁H₁₄BrFN₄O: C, 57.68%; H, 3.23%; N, 12.81%. Found: C, 60.01%; H, 3.52%; N, 13.22%.

4.3.2. *N*-4-((3-Bromophenyl)amino)quinazolin-6-yl)-4-fluorobenzamide (8). Yellow powder, yield: 85%. m.p. 274–276 °C; ^1H NMR (300 MHz, DMSO- d_6 , δ ppm): 7.28–7.45 (m, 4H), 7.82–7.91 (m, 2H), 8.03 (dd, $J_1 = 8.97$ Hz, $J_2 = 8.97$ Hz, 1H), 8.16–8.20 (m, 3H), 8.62 (s, 1H), 8.90 (s, 1H), 9.94 (s, 1H), 10.62 (s, 1H). ^{13}C NMR (300 MHz, DMSO- d_6) δ : 167.46, 165.35, 156.36, 153.13, 148.47, 144.53, 133.47, 130.57, 130.04, 130.01, 129.53, 127.34, 125.34, 124.75, 122.92, 119.03, 115.78, 115.43, 114.23. ESI-MS: 438.2 (C₂₁H₁₅BrFN₄O [M + H]⁺). Anal. calcd for C₂₁H₁₄BrFN₄O: C, 57.68%; H, 3.23%; N, 12.81%. Found: C, 57.23%; H, 3.54%; N, 13.21%.

4.3.3. *N*-4-((3-Bromophenyl)amino)quinazolin-6-yl)-4-nitrobenzamide (9). Yellow powder, yield: 84%. m.p. 237–239 °C; ^1H NMR (300 MHz, DMSO- d_6 , δ ppm): 7.13 (d, $J = 7.12$ Hz, 1H), 7.33 (t, $J = 4.13$ Hz, 1H), 7.65 (t, $J = 4.43$ Hz, 2H), 8.02 (t, $J = 3.11$ Hz, 2H), 8.21 (d, $J = 8.47$ Hz, 1H), 8.32 (t, $J = 6.30$ Hz, 3H), 8.45 (d, $J = 8.48$ Hz, 2H), 8.53 (s, 1H), 8.89 (s, 1H), 9.94 (s, 1H), 10.76 (s, 1H). ^{13}C NMR (300 MHz, DMSO- d_6) δ : 165.34, 153.13, 145.56, 137.67, 133.47, 131.34, 129.56, 129.13, 127.41, 125.47, 124.77, 124.12, 122.87, 120.68, 115.60, 114.32. ESI-MS: 464.3 (C₂₁H₁₅BrN₅O₃ [M + H]⁺). Anal. calcd for C₂₁H₁₄BrN₅O₃: C, 54.33%; H, 3.04%; N, 15.08%. Found: C, 54.63%; H, 3.34%; N, 14.69%.

4.3.4. *N*-(4-((3-Bromophenyl)amino)quinazolin-6-yl)-2-methylbenzamide (10). Yellow powder, yield: 80%. m.p. 252–254 °C; ^1H NMR (300 MHz, DMSO- d_6 , δ ppm): 2.46 (s, 3H, $-\text{CH}_3$), 7.29–7.79 (m, 4H), 7.44 (t, $J = 3.93$ Hz, 1H), 7.53 (d, $J = 1.29$ Hz, 1H), 7.80–7.88 (m, 2H), 7.95 (d, $J = 8.97$ Hz, 1H), 8.32 (s, 1H), 8.60 (s, 1H), 9.97 (s, 1H), 8.93 (s, 1H), 10.65 (s, 1H). ^{13}C NMR (300 MHz, DMSO- d_6) δ : 167.78, 158.45, 152.13, 149.54, 144.67, 137.69, 135.14, 133.47, 131.14, 127.89, 127.13, 124.88, 122.76, 119.79, 115.87, 114.43. ESI-MS: 434.3 ($\text{C}_{22}\text{H}_{18}\text{BrN}_4\text{O} [\text{M} + \text{H}]^+$). Anal. calcd for $\text{C}_{22}\text{H}_{17}\text{BrN}_4\text{O}$: C, 60.98%; H, 3.95%; N, 12.93%. Found: C, 60.57%; H, 4.25%; N, 12.53%.

4.3.5. *N*-(4-((3-Bromophenyl)amino)quinazolin-6-yl)-2-(4-chlorophenyl)acetamide (11). Yellow powder, yield: 89%. m.p. 251–253 °C; ^1H NMR (300 MHz, DMSO- d_6 , δ ppm): 3.76 (s, 2H), 7.26–7.76 (m, 2H), 7.41 (s, 4H), 7.78–7.89 (m, 3H), 8.14 (s, 1H), 8.58 (s, 1H), 8.71 (d, $J = 0.15$ Hz, 1H), 9.90 (s, 1H), 10.54 (s, 1H). ^{13}C NMR (300 MHz, DMSO- d_6) δ : 173.54, 156.28, 153.34, 149.54, 146.01, 134.35, 134.13, 133.41, 130.23, 130.03, 129.68, 129.43, 127.82, 125.71, 125.19, 122.78, 120.46, 115.87, 114.67. ESI-MS: 468.8 ($\text{C}_{22}\text{H}_{17}\text{BrClN}_4\text{O} [\text{M} + \text{H}]^+$). Anal. calcd for $\text{C}_{22}\text{H}_{16}\text{BrClN}_4\text{O}$: C, 56.49%; H, 3.45%; N, 11.98%. Found: C, 56.73%; H, 3.47%; N, 12.05%.

4.3.6. 2-(4-Bromophenyl)-*N*-(4-((3-bromophenyl)amino)quinazolin-6-yl)acetamide (12). Yellow powder, yield: 75%. m.p. 256–258 °C; ^1H NMR (300 MHz, DMSO- d_6 , δ ppm): 3.74 (s, 2H), 7.27–7.41 (m, 4H), 7.55 (d, $J = 8.25$ Hz, 2H), 7.78–7.89 (m, 3H), 8.14 (s, 1H), 8.58 (s, 1H), 8.71 (d, $J = 1.43$ Hz, 1H), 9.90 (s, 1H), 10.53 (s, 1H). ^{13}C NMR (300 MHz, DMSO- d_6) δ : 173.47, 157.29, 153.13, 149.48, 144.53, 134.78, 134.26, 131.53, 130.34, 130.02, 129.81, 127.43, 125.34, 124.87, 122.56, 121.31, 120.78, 115.79, 114.87. ESI-MS: 513.2 ($\text{C}_{22}\text{H}_{17}\text{Br}_2\text{N}_4\text{O} [\text{M} + \text{H}]^+$). Anal. calcd for $\text{C}_{22}\text{H}_{16}\text{Br}_2\text{N}_4\text{O}$: C, 51.59%; H, 3.15%; N, 10.94%. Found: C, 51.67%; H, 3.14%; N, 11.03%.

4.3.7. *N*-(4-((3-Bromophenyl)amino)quinazolin-6-yl)-2-(4-fluorophenyl)acetamide (13). Yellow powder, yield: 82%. m.p. 214–216 °C; ^1H NMR (300 MHz, DMSO- d_6 , δ ppm): 7.18 (t, $J = 4.48$ Hz, 2H), 7.26–7.33 (m, 2H), 7.36–7.44 (m, 2H), 7.78–7.89 (m, 3H), 8.14 (s, 1H), 8.57 (s, 1H), 8.72 (s, 1H), 9.89 (s, 1H), 10.52 (s, 1H). ^{13}C NMR (300 MHz, DMSO- d_6) δ : 172.56, 163.59, 157.34, 152.19, 149.54, 145.53, 133.51, 130.71, 130.13, 129.87, 129.27, 127.32, 125.24, 124.79, 122.86, 120.64, 115.79, 115.14, 114.83, 41.27. ESI-MS: 523.0 ($\text{C}_{22}\text{H}_{17}\text{BrFN}_4\text{O} [\text{M} + \text{H}]^+$). Anal. calcd for $\text{C}_{22}\text{H}_{16}\text{BrFN}_4\text{O}$: C, 52.70%; H, 3.08%; N, 10.69%. Found: C, 52.43%; H, 3.36%; N, 10.89%.

4.3.8. *N*-(4-((3-Bromophenyl)amino)quinazolin-6-yl)picolinamide (14). Yellow powder, yield: 85%. m.p. 263–264 °C; ^1H NMR (300 MHz, DMSO- d_6 , δ ppm): 7.27–7.38 (m, 2H), 7.72 (t, $J = 6.12$ Hz, 1H), 7.83 (d, $J = 8.97$ Hz, 1H), 7.9 (d, $J = 7.86$ Hz, 1H), 8.11 (t, $J = 7.68$ Hz, 1H), 8.22 (d, $J = 7.86$ Hz, 2H), 8.34 (dd, $J_1 = 9.15$ Hz, $J_2 = 8.97$ Hz, 1H), 8.60 (s, 1H), 8.77 (d, $J = 4.74$ Hz, 1H), 8.88 (s, 1H), 9.87 (s, 1H), 10.90 (s, 1H). ^{13}C NMR (300 MHz, DMSO- d_6) δ : 163.57, 157.28, 152.13, 150.63, 150.71, 149.72, 149.42, 144.78, 137.67, 133.46, 141.05, 129.59, 126.47, 124.79, 122.90, 120.64, 115.79, 114.57. ESI-MS: 421.3 ($\text{C}_{20}\text{H}_{15}\text{BrN}_5\text{O} [\text{M} + \text{H}]^+$). Anal. calcd for $\text{C}_{20}\text{H}_{14}\text{BrN}_5\text{O}$: C, 57.16%; H, 3.36%; N, 16.66%. Found: C, 57.27%; H, 3.56%; N, 16.52%.

4.3.9. *N*-(4-((3-Bromophenyl)amino)quinazolin-6-yl)benzamide (15). Yellow powder, yield: 84%. m.p. 275–276 °C; ^1H NMR (300 MHz, DMSO- d_6 , δ ppm): 7.28–7.38 (m, 2H), 7.55–7.64 (m, 3H), 7.82–7.91 (m, 2H), 8.04 (t, $J = 3.57$ Hz, 3H), 8.20 (s, 1H), 8.92 (s, 1H), 9.93 (s, 1H), 10.61 (s, 1H). ^{13}C NMR (300 MHz, DMSO- d_6) δ : 168.56, 157.43, 151.79, 147.89, 144.86, 134.81, 133.46, 131.38, 130.04, 129.39, 128.57, 128.23, 127.73, 125.43, 124.99, 122.73, 119.43, 115.87, 114.21. ESI-MS: 420.2 ($\text{C}_{21}\text{H}_{16}\text{BrN}_4\text{O} [\text{M} + \text{H}]^+$). Anal. calcd for $\text{C}_{21}\text{H}_{15}\text{BrN}_4\text{O}$: C, 60.16%; H, 3.61%; N, 13.36%. Found: C, 60.26%; H, 3.35%; N, 13.71, 13.17%.

4.3.10. *N*-(4-((3-Bromophenyl)amino)quinazolin-6-yl)-4-chlorobenzamide (16). Yellow powder, yield: 79%. m.p. 244–246 °C; ^1H NMR (300 MHz, DMSO- d_6 , δ ppm): 7.07 (d, $J = 8.4$ Hz, 2H), 7.30–7.43 (m, 3H), 7.72–7.86 (m, 2H), 8.04 (d, $J = 8.4$ Hz, 1H), 8.11 (d, $J = 8.4$ Hz, 1H), 8.18 (s, 1H, NH), 8.63 (s, 1H), 8.78 (s, 1H), 10.82 (s, 1H), 11.54 (s, 1H, NHCO). ^{13}C NMR (300 MHz, DMSO- d_6) δ : 167.71, 156.34, 152.13, 149.46, 145.53, 137.81, 135.12, 133.43, 130.02, 129.63, 128.72, 128.31, 127.73, 125.27, 124.52, 121.98, 120.43, 115.90, 114.23. ESI-MS: 454.7 ($\text{C}_{21}\text{H}_{14}\text{BrClN}_4\text{O} [\text{M} \pm \text{H}]^+$). Anal. calcd for $\text{C}_{21}\text{H}_{14}\text{BrClN}_4\text{O}$: C, 55.59%; H, 3.11%; N, 12.35%. Found: C, 55.72%; H, 3.18%; N, 12.14%.

4.3.11. *N*-(4-((3-Bromophenyl)amino)quinazolin-6-yl)-2-(3-chlorophenyl)acetamide (17). Yellow powder, yield: 81%. m.p. 269–271 °C; ^1H NMR (300 MHz, DMSO- d_6 , δ ppm): 3.78 (s, 2H), 7.27–7.42 (m, 5H), 7.47 (s, 1H), 7.78–7.89 (m, 3H), 8.14 (s, 1H), 8.58 (s, 1H), 8.73 (s, 1H), 9.92 (s, 1H), 10.56 (s, 1H). ^{13}C NMR (300 MHz, DMSO- d_6) δ : 172.45, 157.28, 152.23, 148.56, 145.72, 137.78, 134.53, 133.79, 130.14, 129.78, 129.12, 128.89, 127.47, 127.39, 125.36, 124.87, 122.89, 120.66, 115.87, 114.91, 42.98. ESI-MS: 468.8 ($\text{C}_{22}\text{H}_{17}\text{BrClN}_4\text{O} [\text{M} + \text{H}]^+$). Anal. calcd for $\text{C}_{22}\text{H}_{16}\text{BrClN}_4\text{O}$: C, 56.49%; H, 3.45%; N, 11.98%. Found: C, 56.73%; H, 3.49%; N, 12.04%.

4.3.12. *N*-(4-((3-Chlorophenyl)amino)quinazolin-6-yl)-4-fluorobenzamide (18). White powder, yield: 87%. m.p. 284–285 °C; ^1H NMR (300 MHz, DMSO- d_6 , δ ppm): 7.16 (d, $J = 9.12$ Hz, 1H), 7.29–7.45 (m, 3H), 7.84 (d, $J = 8.79$ Hz, 2H), 8.02 (d, $J = 8.97$ Hz, 1H), 8.08–8.16 (m, 3H), 8.62 (s, 1H), 8.89 (s, 1H), 9.95 (s, 1H), 10.63 (s, 1H). ^{13}C NMR (300 MHz, DMSO- d_6) δ : 167.57, 165.79, 157.23, 152.21, 149.53, 144.09, 134.34, 133.46, 130.79, 130.13, 130.01, 129.54, 127.72, 121.78, 120.87, 120.21, 115.90, 115.34, 114.26. ESI-MS: 393.8 ($\text{C}_{21}\text{H}_{15}\text{ClFN}_4\text{O} [\text{M} + \text{H}]^+$). Anal. calcd for $\text{C}_{21}\text{H}_{14}\text{ClFN}_4\text{O}$: C, 64.21%; H, 3.59%; Cl, 9.03%; F, 4.84%; N, 14.26%; O, 4.07%. Found: C, 64.21%; H, 3.59%; N, 14.26%.

4.3.13. *N*-(4-((3-Chlorophenyl)amino)quinazolin-6-yl)-4-nitrobenzamide (19). White powder, yield: 67%. m.p. 319–321 °C; ^1H NMR (300 MHz, DMSO- d_6 , δ ppm): 7.17 (d, $J = 7.32$ Hz, 1H), 7.42 (t, $J = 4.02$ Hz, 1H), 7.85 (t, $J = 4.48$ Hz, 2H), 8.05 (t, $J = 3.02$ Hz, 2H), 8.17 (d, $J = 8.58$ Hz, 1H), 8.30 (t, $J = 6.40$ Hz, 3H), 8.43 (d, $J = 8.58$ Hz, 2H), 8.63 (s, 1H), 8.91 (s, 1H), 9.96 (s, 1H), 10.92 (s, 1H). ^{13}C NMR (300 MHz, DMSO- d_6) δ : 167.57, 157.29, 152.21, 150.16, 149.47, 144.19, 138.63, 134.47, 133.45, 130.21, 129.65, 129.38, 127.69, 124.09, 122.57, 120.98, 120.21, 115.90, 114.23. ESI-MS: 420.8 ($\text{C}_{21}\text{H}_{15}\text{ClN}_5\text{O}_3 [\text{M} + \text{H}]^+$). Anal. calcd for $\text{C}_{21}\text{H}_{14}\text{ClN}_5\text{O}_3$: C, 60.08%; H, 3.36%; N, 16.68%. Found: C, 60.32%; H, 3.34%; N, 16.71%.

4.3.14. *N*-(4-((3-Chlorophenyl)amino)quinazolin-6-yl)-2-methylbenzamide (20). White powder, yield: 83%. m.p. 252–254 °C; ^1H NMR (300 MHz, DMSO- d_6 , δ ppm): 2.45 (s, 3H, $-\text{CH}_3$), 7.32–7.47 (m, 4H), 7.50–7.57 (m, 2H), 7.70 (d, $J = 8.67$ Hz, 1H), 7.89 (t, $J = 1$ Hz, 1H), 8.06 (d, $J = 8.97$ Hz, 1H), 8.16 (dd, $J_1 = 9.12$ Hz, $J_2 = 8.94$ Hz, 1H), 8.90 (s, 1H), 9.22 (s, 1H), 10.94 (s, 1H), 11.58 (s, 1H). ^{13}C NMR (300 MHz, DMSO- d_6) δ : 168.11, 157.29, 151.97, 149.43, 144.12, 138.17, 135.22, 134.41, 133.47, 130.96, 130.14, 129.53, 127.96, 127.69, 127.02, 122.62, 120.89, 120.18, 115.91, 114.21, 20.22. ESI-MS: 389.9 ($\text{C}_{22}\text{H}_{18}\text{ClN}_4\text{O}$ $[\text{M} + \text{H}]^+$). Anal. calcd for $\text{C}_{22}\text{H}_{17}\text{ClN}_4\text{O}$: C, 67.95%; H, 4.41%; N, 14.41%. Found: C, 68.03%; H, 4.40%; N, 14.45%.

4.3.15. 2-(4-Chlorophenyl)-*N*-(4-((3-chlorophenyl)amino)quinazolin-6-yl)acetamide (21). White powder, yield: 81%. m.p. 314–315 °C; ^1H NMR (300 MHz, DMSO- d_6 , δ ppm): 3.79 (s, 2H), 7.14 (d, $J = 6.96$ Hz, 1H), 7.41 (s, 6H), 7.77 (d, $J = 7.50$ Hz, 2H), 7.98 (d, $J = 11.54$ Hz, 2H), 8.56 (s, 1H), 8.74 (s, 1H), 10.01 (s, 1H), 10.97 (s, 1H). ^{13}C NMR (300 MHz, DMSO- d_6) δ : 172.49, 156.97, 152.13, 149.47, 144.12, 134.43, 134.29, 133.97, 133.43, 130.32, 130.15, 129.81, 129.54, 127.36, 122.59, 120.87, 120.21, 115.91, 114.87, 43.45. ESI-MS: 424.2 ($\text{C}_{22}\text{H}_{16}\text{Cl}_2\text{N}_4\text{O}$ $[\text{M} + \text{H}]^+$). Anal. calcd for $\text{C}_{22}\text{H}_{16}\text{Cl}_2\text{N}_4\text{O}$: C, 62.42%; H, 3.81%; N, 13.24%. Found: C, 62.82%; H, 3.81%; N, 13.24%.

4.3.16. 2-(4-Bromophenyl)-*N*-(4-((3-chlorophenyl)amino)quinazolin-6-yl)acetamide (22). Yellow powder, yield: 77%. m.p. 255–257 °C; ^1H NMR (300 MHz, DMSO- d_6 , δ ppm): 3.73 (s, 2H), 7.14 (d, $J = 9.15$ Hz, 1H), 7.33–7.41 (m, 3H), 7.55 (d, $J = 8.22$ Hz, 2H), 7.79 (d, $J = 9.15$ Hz, 2H), 7.87 (d, $J = 10.95$ Hz, 1H), 8.02 (s, 1H), 8.57 (s, 1H), 8.71 (s, 1H), 9.89 (s, 1H), 10.53 (s, 1H). ^{13}C NMR (300 MHz, DMSO- d_6) δ : 172.43, 157.31, 152.09, 149.51, 144.17, 134.43, 134.34, 131.69, 130.21, 130.04, 129.81, 127.34, 122.59, 121.47, 120.91, 120.23, 115.87, 114.89, 43.42. ESI-MS: 468.8 ($\text{C}_{22}\text{H}_{17}\text{BrClN}_4\text{O}$ $[\text{M} + \text{H}]^+$). Anal. calcd for $\text{C}_{22}\text{H}_{16}\text{BrClN}_4\text{O}$: C, 56.49%; H, 3.45%; N, 11.98%. Found: C, 56.61%; H, 3.62%; N, 11.88%.

4.3.17. *N*-(4-((3-Chlorophenyl)amino)quinazolin-6-yl)-2-(4-fluorophenyl)acetamide (23). White powder, yield: 87%. m.p. 248–250 °C; ^1H NMR (300 MHz, DMSO- d_6 , δ ppm): 3.76 (s, 2H), 7.15–7.24 (m, 3H), 7.43 (t, $J = 3.2$ Hz, 3H), 7.73 (d, $J = 8.22$ Hz, 1H), 7.84 (d, $J = 8.97$ Hz, 1H), 7.94 (d, $J = 6.75$ Hz, 2H), 8.68 (s, 1H), 8.83 (s, 1H), 10.44 (s, 1H), 10.71 (s, 1H). ^{13}C NMR (300 MHz, DMSO- d_6) δ : 172.31, 152.23, 149.51, 144.09, 134.43, 134.34, 130.61, 130.43, 130.12, 129.82, 127.41, 122.63, 120.57, 120.18, 115.87, 115.23, 114.76, 43.47. ESI-MS: 407.8 ($\text{C}_{22}\text{H}_{17}\text{ClFN}_4\text{O}$ $[\text{M} + \text{H}]^+$). Anal. calcd for $\text{C}_{22}\text{H}_{17}\text{ClFN}_4\text{O}$: C, 64.95%; H, 3.96%; N, 13.77%. Found: C, 64.95%; H, 3.96%; N, 13.77%.

4.3.18. *N*-(4-((3-Chlorophenyl)amino)quinazolin-6-yl)picolinamide (24). White powder, yield: 84%. m.p. 281–283 °C; ^1H NMR (300 MHz, DMSO- d_6 , δ ppm): 7.17 (d, $J = 8.61$ Hz, 1H), 7.43 (t, $J = 4.03$ Hz, 1H), 7.72–7.76 (m, 1H), 7.85 (d, $J = 8.97$ Hz, 2H), 8.10–8.16 (m, 2H), 8.24 (d, $J = 7.68$ Hz, 1H), 8.37 (dd, $J_1 = 8.97$ Hz, $J_2 = 9.15$ Hz, 1H), 8.63 (s, 1H), 8.80 (d, $J = 4.56$ Hz, 1H), 8.91 (d, $J = 2.01$ Hz), 9.91 (s, 1H), 10.92 (s, 1H). ^{13}C NMR (300 MHz, DMSO- d_6) δ : 165.17, 157.31, 152.21, 150.45, 149.47, 149.34, 144.09, 137.85, 134.45, 133.71, 130.23, 129.54, 127.75, 127.56, 127.09, 122.45, 120.91, 120.21, 115.87, 114.27. ESI-MS: 376.8

($\text{C}_{20}\text{H}_{15}\text{ClN}_5\text{O}$ $[\text{M} + \text{H}]^+$). Anal. calcd for $\text{C}_{20}\text{H}_{14}\text{ClN}_5\text{O}$: C, 63.92%; H, 3.75%; N, 18.64%. Found: C, 64.02%; H, 3.85%; N, 17.96%.

4.3.19. *N*-(4-((3-Chlorophenyl)amino)quinazolin-6-yl)-3,4-diethoxybenzamide (25). White powder, yield: 83%. m.p. 279–281 °C; ^1H NMR (300 MHz, DMSO- d_6 , δ ppm): 3.68 (m, 4H), 4.00 (m, 6H), 6.90 (s, 2H), 7.00 (s, 1H), 7.37 (d, $J = 7.32$ Hz, 1H), 7.50 (t, $J = 4.11$ Hz, 1H), 7.64 (d, $J = 8.04$ Hz, 1H), 7.85 (s, 1H), 7.94 (d, $J = 8.97$ Hz, 1H), 8.05 (d, $J = 9.15$ Hz, 1H), 8.88 (s, 1H), 9.01 (s, 1H), 10.84 (s, 1H), 11.37 (s, 1H). ^{13}C NMR (300 MHz, DMSO- d_6) δ : 167.11, 157.29, 152.43, 152.14, 150.73, 149.47, 144.09, 134.43, 133.63, 130.21, 129.57, 129.32, 127.72, 122.54, 122.33, 120.87, 120.11, 115.87. ESI-MS: 463.9 ($\text{C}_{25}\text{H}_{23}\text{ClN}_4\text{O}_3$ $[\text{M} + \text{H}]^+$). Anal. calcd for $\text{C}_{25}\text{H}_{23}\text{ClN}_4\text{O}_3$: C, 64.86%; H, 5.01%; N, 12.10%. Found: C, 64.94%; H, 5.21%; N, 12.08%.

4.4. c-Src kinase assay

A coupled spectrophotometric assay was used wherein ADP generated by c-Src kinase was converted to ATP by pyruvate kinase (PK), with concomitant production of pyruvate from phosphoenolpyruvate (PEP).³³ LDH reduces pyruvate to lactate by oxidizing NADH. NADH depletion was monitored at 340 nm using a microplate reader (Spectra Max 250, Molecular Device) at 30 °C for 20 min. Reactions were performed at 30 °C in 100 mM Hepes buffer (pH 7.6), containing 20 mM MgCl_2 and 10% glycerol, initiated by adding ATP. PK (100 $\mu\text{g mL}^{-1}$), LDH (50 $\mu\text{g mL}^{-1}$), PEP (2 mM), and NADH (140 μM) were also added. Kinase activity was measured by adding 100 μM c-Src optimal peptide substrate (peptide sequence: AEEIYGEFEAKKKK, Sawady, Tokyo).

4.5. Cell proliferation assay

CCK8 is much more convenient and helpful than MTT for analyzing cell proliferation, because it can be reduced to soluble formazan by dehydrogenase in mitochondria and has little toxicity to cells. Cell proliferation was determined using CCK8 dye (Beyotime Inst Biotech, China) according to manufacture's instructions. Briefly, 5×10^3 cells per well were seeded in a 96-well plate, grown at 37 °C for 12 h. Subsequently, cells were treated with compounds at increasing concentrations in the presence of 10% FBS for 24 or 48 h. After 10 μL CCK8 dye was added to each well, cells were incubated at 37 °C for 1–2 h and plates were read in a Victor-V multilabel counter (Perkin-Elmer) using the default europium detection protocol. Percent inhibition or IC_{50} values of compounds were calculated by comparison with DMSO-treated control wells. The results were shown in Table 2.

4.6. Multiple protein kinases assays

The kinase activity of various tyrosine kinases was determined by ELISA.²² EIA/RIA strip-well plates (Corning) were coated with poly(Glu/Tyr, 4 : 1) peptide (Sigma, 50 $\mu\text{g mL}^{-1}$, 100 μL per well) by incubation overnight at 4 °C in phosphate-buffered saline (PBS, Ca/Mg-free). Kinase reaction was performed in the plates by addition of 50 μL kinase buffer (50 mM Hepes, 125 mM NaCl,

10 mM MgCl₂, pH 7.4) containing ATP, 10 ng protein kinases (c-Src, EGFR, CDK2, PTK2, JAK2), and compound **24**. After 20 min, the plates were washed three times with wash buffer (0.1% Tween 20 in PBS) and incubated for 20 min with HRP conjugated anti-phosphotyrosine antibody (0.2 µg mL⁻¹, 50 µL per well, Santa Cruz). After two washes, the plates were developed by the addition of tetramethylbenzidine (50 µL per well, Sigma) and stopped by addition of H₂SO₄ (2 N, 50 µL per well). The absorbance at 450 nm was measured by a 96-well plate reader (Tecan).

4.7. Acute oral toxicity

Five thousand milligrams of compound **24** per kilogram of body weight was administered to ten healthy rats by oral gavage. The animals were observed for mortality, signs of gross toxicity and behavioral changes at least once daily for 14 days. Body weights were recorded prior to administration and again on Day 7 and 14. All animals survived and appeared active and healthy throughout the study. With the exception of one male that exhibited a loss in body weight between Day 7 and 14, all animals gained body weight over the 14-day observation period. There were no signs of gross toxicity or abnormal behavior.

4.8. Experimental protocol of docking study

Molecular docking of compound **24** (or Saracatinib) into the three dimensional X-ray structure of human c-Src (PDB code: 3F3V) was carried out using the Discovery Studio (version 3.5) as implemented through the graphical user interface DS-CDOCKER protocol. The three-dimensional structures of the aforementioned compounds were constructed using Chem. 3D ultra 12.0 software [Chemical Structure Drawing Standard; Cambridge Soft corporation, USA (2010)], then they were energetically minimized by using MMFF94 with 5000 iterations and minimum RMS gradient of 0.10. The crystal structures of protein complex were retrieved from the RCSB Protein Data Bank (<http://www.rcsb.org/pdb/home/home.do>) and prepared (by Discovery Studio 3.5) with all bound waters and ligands eliminated from the protein and the polar hydrogen added to the protein. Molecular docking of all 19 compounds was then carried out using the Discovery Studio (version 3.5) as implemented through the graphical user interface CDOCKER protocol. CDOCKER is an implementation of a CHARMM based molecular docking tool using a rigid receptor.

4.9. 3D-QSAR

Ligand-based 3D-QSAR approach was performed by QSAR software of DS 3.5 (Discovery Studio 3.5, Accelrys, Co. Ltd). The training sets were composed of 15 inhibitors with the corresponding pIC₅₀ values which were converted from the obtained IC₅₀ (µM), and test sets comprised 4 compounds of data sets as list in Table 4. All the definition of the descriptors can be seen in the "Help" of DS 3.5 software and they were calculated by QSAR protocol of DS 3.5. The alignment conformation of each molecule was the one with the lowest interaction energy in the docked results of CDOCKER (generated in Section 4.9). The predictive ability of 3D-QSAR modeling can be evaluated based

on the cross-validated correlation coefficient, which qualifies the predictive ability of the models. Scrambled test (Y scrambling) was performed to investigate the risk of chance correlations. The inhibitory potencies of compounds were randomly reordered for 30 times and subject to leave-one-out validation test, respectively. The models were also validated by test sets, in which the compounds are not included in the training sets. Usually, one can believe that the modeling is reliable, when the *R*² for test sets is larger than 0.6, respectively.

Acknowledgements

This work was supported by the National Forestry Commonweal Project (200904001) and by the Fundamental Research Funds for the Central Universities (1082020803).

Notes and references

- 1 R. Thaimattam, P. R. Daga, R. Banerjee and J. Iqbal, *Bioorg. Med. Chem.*, 2005, **13**, 4704–4712.
- 2 R. Capdeville, E. Buchdunger, J. Zimmermann and A. Matter, *Nat. Rev. Drug Discovery*, 2002, **1**, 493–502.
- 3 N. Nam, S. Lee, G. Ye, G. Sun and K. Parang, *Bioorg. Med. Chem.*, 2004, **12**, 5753–5766.
- 4 J. Dowell, J. D. Minna and P. Kirkpatrick, *Nat. Rev. Drug Discovery*, 2005, **4**, 13–14.
- 5 J. Graham, M. Muhsin and P. Kirkpatrick, *Nat. Rev. Drug Discovery*, 2004, **3**, 11–12.
- 6 X. Cao, Q. You, Z. Li, Q. Guo, J. Shang, M. Yan, J. Chern and M. Chen, *Bioorg. Med. Chem.*, 2008, **16**, 5890–5898.
- 7 S. M. Thomas and J. S. Brugge, *Annu. Rev. Cell Dev. Biol.*, 1997, **13**, 513–609.
- 8 S. J. Parsons and J. T. Parsons, *Oncogene*, 2004, **23**, 7906–7909.
- 9 Y. Liu, K. Shah, F. Yang, L. Witucki and K. M. Shokat, *Bioorg. Med. Chem.*, 1998, **6**, 1219–1226.
- 10 H. Huang, Q. Jia, J. Ma, G. Qin, Y. Chen, Y. Xi, L. Lin, W. Zhu, J. Ding and H. Jiang, *Eur. J. Med. Chem.*, 2009, **44**, 1982–1988.
- 11 T. J. Yeatman, *Nat. Rev. Cancer*, 2004, **4**, 470–480.
- 12 J. M. Summy and G. E. Gallick, *Cancer Metastasis Rev.*, 2003, **22**, 337–358.
- 13 B. F. Boyce, L. Xing, Z. Yao, T. Yamashita, W. C. Shakespeare, Y. Wang, C. A. Metcalf, R. Sundaramoorthi, D. C. Dalgarno and J. D. Iulucci, *Clin. Cancer Res.*, 2006, **12**, 6291s–6295s.
- 14 J. M. Summy and G. E. Gallick, *Cancer Metastasis Rev.*, 2003, **22**, 337–358.
- 15 J. D. Bjorge, A. Jakymiw and D. J. Fujita, *Oncogene*, 2000, **19**, 5620.
- 16 R. B. Irby, W. Mao, D. Coppola, J. Kang, J. M. Loubeau, W. Trudeau, R. Karl, D. J. Fujita, R. Jove and T. J. Yeatman, *Nat. Genet.*, 1999, **21**, 187–190.
- 17 D. Berger, M. Dutia, D. Powell, B. Wu, A. Wissner, D. H. Boschelli, M. B. Floyd, N. Zhang, N. Torres and J. Levin, *Bioorg. Med. Chem. Lett.*, 2003, **13**, 3031–3034.
- 18 B. Boyer, A. M. Vallés and N. Edme, *Biochem. Pharmacol.*, 2000, **60**, 1091–1099.

- 19 B. Barlaam, M. Fennell, H. Germain, T. Green, L. Hennequin, R. Morgentin, A. Olivier, P. Plé, M. Vautier and G. Costello, *Bioorg. Med. Chem. Lett.*, 2005, **15**, 5446–5449.
- 20 I. Pevet, C. Brulé, A. Tizot, A. Gohier, F. Cruzalegui, J. A. Boutin and S. Goldstein, *Bioorg. Med. Chem.*, 2011, **19**, 2517–2528.
- 21 D. M. Berger, M. Dutia, G. Birnberg, D. Powell, D. H. Boschelli, Y. D. Wang, M. Ravi, D. Yaczko, J. Golas and J. Lucas, *J. Med. Chem.*, 2005, **48**, 5909–5920.
- 22 W. D. Klohs, D. W. Fry and A. J. Kraker, *Curr. Opin. Oncol.*, 1997, **9**, 562–568.
- 23 R. L. Dow, B. M. Bechle, T. T. Chou, C. Goddard and E. R. Larson, *Bioorg. Med. Chem. Lett.*, 1995, **5**, 1007–1010.
- 24 J. H. Hanke, J. P. Gardner, R. L. Dow, P. S. Changelian, W. H. Brissette, E. J. Weringer, B. A. Pollok and P. A. Connelly, *J. Biol. Chem.*, 1996, **271**, 695–701.
- 25 E. B. Haura, T. Tanvetyanon, A. Chiappori, C. Williams, G. Simon, S. Antonia, J. Gray, S. Litschauer, L. Tetteh and A. Neuger, *J. Clin. Oncol.*, 2010, **28**, 1387–1394.
- 26 J. F. Vansteenkiste, *Expert Rev. Anticancer Ther.*, 2004, **4**, 5–17.
- 27 A. J. Barker, K. H. Gibson, W. Grundy, A. A. Godfrey, J. J. Barlow, M. P. Healy, J. R. Woodburn, S. E. Ashton, B. J. Curry and L. Scarlett, *Bioorg. Med. Chem. Lett.*, 2001, **11**, 1911–1914.
- 28 F. A. Shepherd, J. Rodrigues Pereira, T. Ciuleanu, E. H. Tan, V. Hirsh, S. Thongprasert, D. Campos, S. Maoleekoonpiroj, M. Smylie and R. Martins, *N. Engl. J. Med.*, 2005, **353**, 123–132.
- 29 G. W. Rewcastle, W. A. Denny, A. J. Bridges, H. Zhou, D. R. Cody, A. McMichael and D. W. Fry, *J. Med. Chem.*, 1995, **38**, 3482–3487.
- 30 H. Tsou, N. Mamuya, B. D. Johnson, M. F. Reich, B. C. Gruber, F. Ye, R. Nilakantan, R. Shen, C. Discifani and R. DeBlanc, *J. Med. Chem.*, 2001, **44**, 2719–2734.
- 31 D. D. Li, F. Fang, J. R. Li, Q. R. Du, J. Sun, H. B. Gong and H. L. Zhu, *Bioorg. Med. Chem. Lett.*, 2012, **22**, 5870–5875.
- 32 G. Wu, D. H. Robertson, C. L. Brooks and M. Vieth, *J. Comput. Chem.*, 2003, **24**, 1549–1562.
- 33 H. Mukaiyama, T. Nishimura, S. Kobayashi, T. Ozawa, N. Kamada, Y. Komatsu, S. Kikuchi, H. Oonota and H. Kusama, *Bioorg. Med. Chem.*, 2007, **15**, 868–885.
- 34 A. G. Villasenor, R. Kondru, H. Ho, S. Wang, E. Papp, D. Shaw, J. W. Barnett, M. F. Browner and A. Kuglstat, *Chem. Biol. Drug Des.*, 2009, **73**, 466–470.
- 35 A. G. Villasenor, R. Kondru, H. Ho, D. Shaw, J. W. Barnett and A. Kuglstat, *Chem. Biol. Drug Des.*, 2012, **80**, 324–329.